NEW MEMBRANE CONCEPT APPLIED TO THE ANALYSIS OF FLUID SHEAR- AND MICROPIPETTE-DEFORMED RED BLOOD CELLS

E. A. EVANS

From the Department of Engineering Physics, McMaster University, Hamilton, Ontario, Canada. Dr. Evans's present address is the Department of Biomedical Engineering, Duke University, Durham, North Carolina 27706.

ABSTRACT A two-dimensional elastomer material concept of the red cell membrane is applied to the analysis of fluid shear-deformed, point-attached red cells and micropipette aspiration of red cell disks. The elastic constant (corresponding to the "shear" modulus multiplied by the membrane thickness) is of the order 10^{-2} dyn/cm for both cases. Additional experimental observations are in agreement with the membrane model, e.g. teardrop and "tether" formation of the sheared disks, pressure difference vs. aspirated length of the cell for micropipette experiments, etc

INTRODUCTION

The material properties of the red blood cell membrane are of important interest to biological scientists, bioengineers, and clinical hematologists alike. It is generally accepted that the red cell interior is in the liquid state; therefore, the elastic recovery of the red cell is associated with its membrane. There have been numerous experiments to measure the elastic constants of the red cell membrane. Unfortunately, the different experiments have yielded widely varying results, e.g., from 10^4 to 10^8 dyn/cm^2 for the modulus of elasticity. The difficulties of creating and measuring forces and deformations on a biconcave disk (the normal red cell) with a diameter of 8 μm and maximum thickness of 2.5 μm are obviously significant. The three most familiar approaches are osmotic swelling (Fung and Tong, 1968; Evans, 1973), fluid shear deformation of attached cells (Hochmuth and Mohandas, 1972), and micropipette suction (Rand and Burton, 1964). An apparent contradictory behavior exists between the first approach and the latter two. The osmotically swollen cells are very rigid near the spherical state. On the other hand, large deformations are observed for attached cells that are deformed by fluid shear and for normal cells aspirated into small micropipettes.

Recently, a new material concept for the red cell membrane was introduced that provides the capability of large deformations exhibited by normal discocytes and

yet the rigidity of osmotic spherocytes (Evans, 1973). The model of the membrane as a two-dimensional, incompressible material was proposed and a general stress-strain law was developed for finite deformations.[1] The composite molecular character of such a material would resemble a two-dimensional matrix of long chains, randomly kinked and cross-linked in the natural state (analogous to a three-dimensional elastomer), with an interstitial liquid phase. The material would resist uniform dilatation, storing energy in the form of membrane tension, but could easily stretch in any direction with a commensurate shortening in the other dimension. The spheroidal, osmotically swollen state was considered using this model; because there is no method for accurately measuring the internal pressure of the cell near the spherical state, the discocyte-to-osmotic spherocyte transformation cannot provide a good estimate of the elastic constant. Therefore the purpose of this paper is to analyze and compare the results of the other two experimental measurements using the new material proposition.

SHEAR-DEFORMED POINT-ATTACHED RED CELLS

Hochmuth and Mohandas (1972) have published some interesting results on fluid shear-deformed, attached red cells. They chose cells with single-point and double-point attachments. Here, only the single-point-attached cells will be considered. There are four significant observations that must be explained: (*a*) the teardrop shape of the deformed cells; (*b*) reduction in cross section with extension in length (the product of the length ratios was approximately unity); (*c*) the "tethering" phenomenon; and (*d*) the nonlinear character of the stress-strain curve. The deformation of the cell is modeled as a two-dimensional, shear deformation of a thin, circular disk. Obviously, this is only a rough approximation to the actual situation, but it will provide an interesting correlation with the first three observations.

The material element defined by $(x_0, x_0 + \mathrm{d}x_0)$ in Fig. 1 is deformed into the element $(x, x + \mathrm{d}x)$ under the action of the uniform shear stress τ_0. The unilateral extension of the element yields the following force balance involving the stress resultants in the x, y directions,

$$T_y = 0.$$

$$2\mathrm{d}[T_x Y(x)] = \tau_0 \,\mathrm{d}A, \tag{1}$$

where $Y(x)$ is the half-width of the element $\mathrm{d}A$. The first equation is recognized not to be the boundary condition at the edge of a solid circular disk, but rather an ap-

[1] After the article by Evans (1973) was submitted for review, a similar development by Skalak et al. appeared in the March 1973 issue of the *Biophysical Journal*. The general theoretical development is the same however there are some significant differences in final stress-strain laws (see Appendix of Evans [1973]). The two-dimensional, incompressible case was briefly mentioned by Skalak et al. but not explicitly treated.

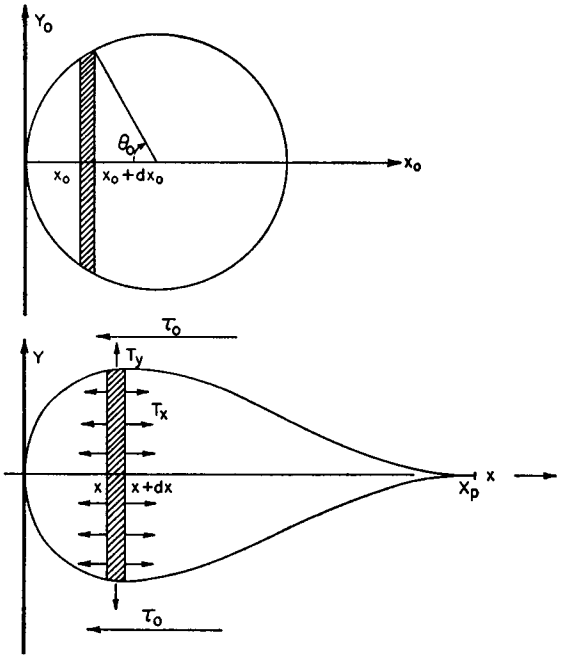

FIGURE 1 Schematic illustration of the deformation of an element defined by $(x_0, x_0 + dx_0)$ into the element $(x, x + dx)$ under the action of a uniform fluid shear stress, τ_0. X_p is the point of attachment.

proximation reflecting the condition that the element dA is a flattened cylindrical "hoop" possessing much larger curvature at the edge in comparison with the curvature in the circumferential direction and thereby having an approximately zero hoop stress. Obviously, as the cell is stretched and begins to build up internal pressure, the hoop element will become more circular and the approximation will be invalid. As is shown in Fig. 1, X_p is the point of attachment. Eq. 1 can be integrated to give,

$$2T_x = \tau_0[A(x)/Y(x)]. \tag{2}$$

The finite strains associated with the deformation of element dA are related to the extension ratios,

$$\lambda_x = (dx/dx_0),$$

$$\lambda_y = (Y/Y_0). \tag{3}$$

Lagrangian strains will be used based on the metric of the undeformed element (it is necessary to make the distinction between metrics for finite strains, Prager [1961]).

The principal strains, ϵ_x and ϵ_y, can be expressed in terms of Eq. 3,

$$\epsilon_x = \tfrac{1}{2}(\lambda_x^2 - 1),$$
$$\epsilon_y = \tfrac{1}{2}(\lambda_y^2 - 1). \tag{4}$$

Now, the assumption that the material is two-dimensional, incompressible is introduced. The incompressibility is given by $\lambda_x\lambda_y = 1$. As was shown previously (Evans, 1973), the stress-strain law is,

$$T_x = -p_M + \mu\epsilon_x,$$
$$T_y = -p_M + \mu\epsilon_y, \tag{5}$$

where p_M is a locally isotropic tension analogous to hydrostatic pressure and μ is the elastic constant (which may be a nonlinear function of $\epsilon_x\epsilon_y$ [Evans, 1973]).

Using the first of Eq. 1, the membrane tension can be eliminated and the stress resultant found as a function of the strains,

$$-p_M = -\mu\epsilon_y,$$
$$T_x = \mu(\epsilon_x - \epsilon_y). \tag{6}$$

In addition, p_M includes the additive constant for interfacial surface tension, γ (surface free energy per unit surface area), that results from chemical discontinuity between the membrane and the environmental solutions (Evans, 1973). Therefore, the surface tension need not be considered in the problem.

The incompressibility condition, Eqs. 2, 4, and 6 give the following result,

$$(\lambda_x^2 - \lambda_x^{-2}) = \tau_0 A(x)/\mu Y(x). \tag{7}$$

Eq. 7 can be expressed in terms of the undeformed coordinates (x_0, Y_0) and also in dimensionless form,

$$(\lambda_x^2 - \lambda_x^{-2}) = \frac{\tau_0 R_0}{\mu}\lambda_x \frac{\bar{A}(x_0)}{\bar{Y}_0(x_0)}, \tag{8}$$

noting that,

$$Y(x) = Y_0(x_0)/\lambda_x,$$
$$\bar{Y}_0 = R_0^{-1}Y_0,$$
$$\bar{X}_0 = R_0^{-1}x_0,$$
$$\bar{A} = R_0^{-2}A,$$

and R_0 is the radius of the undeformed disk. As previously stated, the elastic constant

μ is a function of the strain product $\epsilon_x\epsilon_y$; however, for simplicity, the material will be assumed linear, μ is constant.

The new coordinates and nondimensional area can be expressed in terms of the polar angle θ_0 of the undeformed disk.

$$\bar{Y}_0 = \sin\theta_0$$

$$\bar{X}_0 = 1 - \cos\theta_0$$

$$\bar{A}(\theta_0) = \theta_0 - (\sin 2\theta_0/2).$$

Eq. 8 becomes,

$$(\lambda_x - \lambda_x^{-3}) = \frac{\tau_0 R_0}{\mu} \frac{[\theta_0 - (\sin 2\theta_0)/2]}{\sin\theta_0}. \tag{9}$$

The extension ratio λ_x approaches infinity as θ_0 approaches π. Investigating this singularity, we find that,

$$\lambda_x \to (\tau_0 R_0/\mu)(\pi/\bar{\theta}),$$

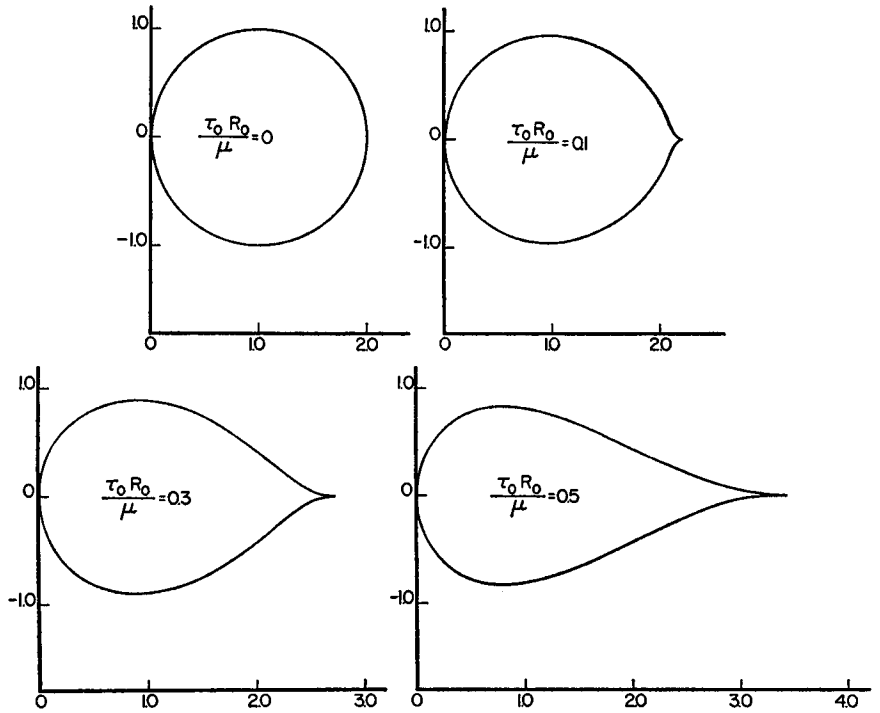

FIGURE 2 The teardrop shape and beginning tether formation of a fluid shear-deformed disk is shown as a function of the dimensionless ratio $\tau_0 R_0/\mu$.

$$\bar{Y} = \bar{Y}_0/\lambda_x \rightarrow (\mu/\pi\tau_0 R_0)\bar{\theta}^2$$

$$d\bar{x} = \lambda_x \, d\bar{x}_0 \rightarrow (\tau_0 R_0 \pi/\mu) \, d\bar{\theta} \tag{10}$$

where $\bar{\theta} = \pi - \theta_0 \rightarrow 0$.

The optical diffraction limit is of the order of 0.5 μm; at this limit, $\bar{Y}$ would equal approximately 0.1. The distance between the point $\bar{Y} = 0.1$ and $\bar{Y} = 0$(at X_p) is obtained from Eqs. 10.

$$\bar{X}_T \simeq 0.3(\pi\tau_0 R_0/\mu)^{3/2}. \tag{11}$$

For the thin disk, therefore, the dimensionless tethering distance would be proportional to the fluid shear stress to the $\frac{3}{2}$ power.

Fig. 2 illustrates the teardrop shape created by the fluid shear stress. The shape is specified by the dimensionless ratio $\tau_0 R_0/\mu$. Fig. 3 contains plots of the extension ratio λ_x vs. the x coordinate of the deformed disk. Finally, Fig. 4 is a plot of $\tau_0 R_0/\mu$ against the total length to original length ratio, excluding the tether length. The tether length is excluded because it would not be observable unless the point of attachment was known.

The final question of nonlinearity of the stress, length ratio observation is not easily answered. The forces normal to the membrane are important in this case because the curvature is appreciable; therefore, such a simple approach as taken

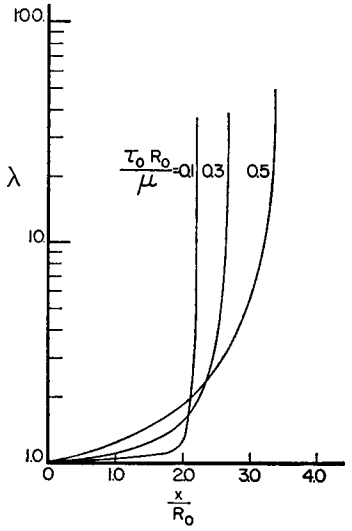

FIGURE 3

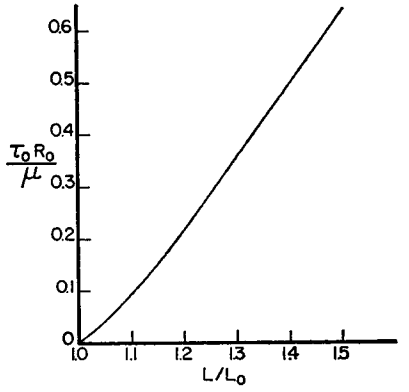

FIGURE 4

FIGURE 3 The principal extension ratio λ_x is plotted against the dimensionless coordinate $\bar{x}$ of the deformed disk for three values of the ratio $\tau_0 R_0/\mu$.

FIGURE 4 The dimensionless ratio $\tau_0 R_0/\mu$ is shown as a function of the total length to original length ratio (excluding the tether length).

here is not valid. For low values of the fluid shear stress, the model provides a useful correlation. Using the data of Hochmuth and Mohandas (1972) and recent data to be published by Hochmuth, a value of the order of 10^4 dyn/cm is obtained for μ. If the membrane thickness is taken as 100 Å then the equivalent elastic modulus would be 10^4 dyn/cm^2. This is the same order as estimated by Hochmuth.

MICROPIPETTE ASPIRATION OF DISCOCYTES

Implementing, for red cells, the approach of Mitchison and Swann (1954), Rand and Burton (1964), and Rand (1964) studied the pressure differential required to aspirate single red cells into small micropipettes. Fig. 5 illustrates the evolution of the process for normal discocytes. They used a liquid drop analogy (law of Laplace) to analyze the results. To Rand and Burton, this was consistent with the linear relationship between pressure difference and the inverse of the pipette radius R_p measured at the condition where $D_p = R_p$ (Fig. 5). What they were unable to explain was that for distances greater than the "critical" point ($D_p = R_p$), the pressure difference required also increased. For a liquid interface, after the critical point, no additional pressure difference is required to draw in the droplet. In addition, they observed that when the portion of the cell outside the micropipette became spherical, further increase in pressure resulted in the "pinching off" of a small globule (illustrated in Fig. 5) or hemolysis.

The suction of an infinite plane membrane into a cylindrical pipette will be taken as the model for the experiment (Fig. 6). The model is valid for small pipettes, for thin discocytes aspirated in the central region, for nonspherical outside portion, and if no buckling occurs. With large pipettes and especially when aspirating the cell at the equator, the cells buckle and "fold" into the pipette. Additional experimental problems exist concerning static and viscous frictional effects, compliance, and leaks in the system that cannot be considered here. For the axisymmetric mem-

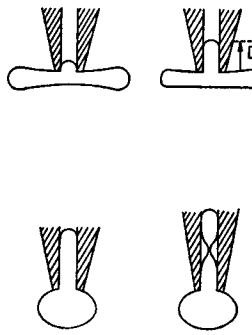

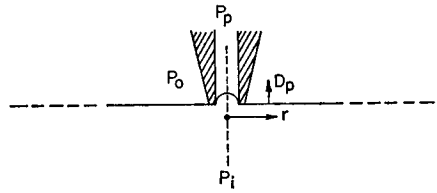

FIGURE 5

FIGURE 6

FIGURE 5 The evolution of a micropipette aspirated, red cell disk is schematically illustrated. D_p is the length of the aspirated tongue.

FIGURE 6 The model of the membrane region surrounding the pipette tip is shown with the critical cap formed in the mouth of the pipette.

brane, the stress resultants in the meridian or radial and azimuthal directions are needed [signified by the respective coordinates (r, θ)] as developed by Flügge (1966). Three problems must be investigated: the formation of the cap, the cap plus the cylindrical section, and the outside plane.

The equations of equilibrium for the stress resultants in the cap are given as (Flügge, 1966),

$$K_s T_s + K_\theta T_\theta = P_i - P_p,$$

$$(\mathrm{d}/\mathrm{d}s)(rT_s) - T_\theta(\mathrm{d}r/\mathrm{d}s) = 0, \tag{12}$$

where s is the curvilinear coordinate along the meridian, and K_s and K_θ are the principal curvatures. (For discussion of the assumptions implicit in the membrane equations and their justification, see Fung and Tong [1968].) Eqs. 12 can be solved to give,

$$T_s = \frac{(P_i - P_p)}{2K_\theta},$$

$$T_\theta = \frac{(2K_\theta - K_s)}{2K_\theta^2}(P_i - P_p). \tag{13}$$

The equilibrium equation for the cylindrical portion in contact with the micropipette inner wall is expressed by,

$$T_s = \text{constant}. \tag{14}$$

The relation assumes that there are no static frictional forces between the membrane and micropipette. The forces normal to the cylinder are balanced by the rigid pipette wall and the fluid film between the membrane and the wall. The hoop stress T_θ/R_p is less than $(P_i - P_p)$; therefore, the membrane will be kept against the pipette wall unless the outside portion of the cell becomes spherical. When the outside portion spheres, no further surface can be drawn into the pipette. Increasing the pressure difference would result in elongation of the cylinder generator with constriction or necking down of the circumference, thereby producing a "pinch off" globule (as illustrated in Fig. 5) observed by Rand (1964). If the cell was initially swollen so that a cylinder could not be formed in the pipette, then the aspirated cap could not neck down and the cell would eventually lyse.

The stress-strain law, Eqs. 5, is now introduced,

$$T_s = -p_M + \mu\epsilon_s,$$

$$T_\theta = -p_M + \mu\epsilon_\theta, \tag{15}$$

and

$$\epsilon_s = \tfrac{1}{2}(\lambda_s^2 - 1),$$

$$\epsilon_\theta = \tfrac{1}{2}(\lambda_s^{-2} - 1), \tag{16}$$

where lagrangian strains have been expressed in terms of the extension ratio relative to the curvilinear coordinate s, using the incompressibility relation.

The extension ratio λ_s is given by the ratio of the undeformed circle circumference to the deformed circle circumference at the same material location.

$$\lambda_s = r_0/r. \tag{17}$$

The radius r in the deformed system is related to the radius r_0 in the initial state by the incompressibility relation,

$$\pi r_0^2 = A_{CAP} + A_{CYL} + \pi(r^2 - R_p^2), \tag{18}$$

where A_{CAP} is the surface area of the cap; A_{CYL} is the surface of the cylinder portion; and R_p is the pipette radius.

The equilibrium equation for the plane outside the pipette is obtained from Eqs. 12 by noting that $dr = ds$, $K_s = K_\theta = 0$, and $P_i = P_0$.

$$(T_s - T_\theta) + r(dT_s/dr) = 0. \tag{19}$$

In terms of Eqs. 15–17, Eq. 19 becomes,

$$\tfrac{1}{2}[(r_0/r)^2 - (r/r_0)^2] + [(r/2)(d/dr)(r_0/r)^2] - (r/\mu)(dp_M/dr) = 0. \tag{20}$$

For the plane region outside the pipette, $r\,dr = r_0\,dr_0$ and Eq. 20 is,

$$2 - [(r_0/r)^2 + (r/r_0^2)] = (2r/\mu)(dp_M/dr). \tag{21}$$

Define,

$$\bar{A}_p = (A_{CAP} + A_{CYL} - \pi R_p^2)/\pi. \tag{22}$$

Using Eqs. 18 and 22, Eq. 21 can be integrated to yield,

$$\left[\frac{\bar{A}_p}{2r^2} - \frac{1}{2}\ln\left(1 + \frac{\bar{A}_p}{r^2}\right)\right]_{\infty}^{R_p} = 2\frac{p_M(R_p) - p_M(\infty)}{\mu}. \tag{23}$$

If the outside portion of the cell does not become spheroidal and remains essentially relaxed, then the value of $p_M(\infty)$ can be taken as zero.

$$\frac{\bar{A}_p}{2R_p^2} - \frac{1}{2}\ln\left(1 + \frac{\bar{A}_p}{R_p^2}\right) = 2\frac{p_M(R_p)}{\mu}. \tag{24}$$

The stress resultants at the micropipette tip (junction of the cylindrical section and the plane) are given by,

$$\frac{T_s}{\mu} = \frac{1}{4}\left[\frac{\bar{A}_p}{R_p^2} + \ln\left(1 + \frac{\bar{A}_p}{R_p^2}\right)\right],$$

$$\frac{T_\theta}{\mu} = \frac{1}{4}\left[\ln\left(1 + \frac{\bar{A}_p}{R_p^2}\right) - \frac{\bar{A}_p}{R_p^2}\frac{3 + (\bar{A}_p/R_p^2)}{1 + (\bar{A}_p/R_p^2)}\right]. \tag{25}$$

In the cylindrical section, T_s is constant and p_M varies to maintain T_s constant,

$$\frac{T_s}{\mu} = \frac{-p_M}{\mu} + \frac{1}{2}\left[\frac{2L}{R_p} + \frac{A_{CAP}}{\pi R_p^2} - 1\right] = \frac{1}{4}\left[\frac{\bar{A}_p}{R_p^2} + \ln\left(1 + \frac{\bar{A}_p}{R_p^2}\right)\right],$$

$$\frac{T_\theta}{\mu} = \left[\frac{1}{4}\ln\left(1 + \frac{\bar{A}_p}{R_p^2}\right) + \frac{\bar{A}_p}{R_p^2} - \frac{4L}{R_p} - \frac{2A_{CAP}}{\pi R_p^2} + 4 \Big/ \left(\frac{4L}{R_p} + \frac{2A_{CAP}}{\pi R_p^2}\right)\right], \quad (26)$$

where L is the coordinate along the cylinder generator, starting from the cap.

At the cap-cylinder junction, the stress resultant T_s is,

$$T_s = \frac{(P_i - P_p)R_p}{2}, \qquad (K_\theta = 1/R_p),$$

and from Eq. 26,

$$\frac{\bar{A}_p}{R_p^2} + \ln\left(1 + \frac{\bar{A}_p}{R_p^2}\right) = 2\,\frac{(P_i - P_p)}{\mu} R_p. \quad (27)$$

Eq. 27 expresses the relationship beween the area of the aspirated "tongue" and the pressure differential required to form the tongue. In order to simply evaluate the equation in terms of the length D_p, assume that the cap is spheroidal (half-ellipse in cross section).

$$A_{CAP} = \pi R_p\left[R_p + \frac{C^2}{(R_p^2 - C^2)^{1/2}} \ln\left(\frac{R_p + (R_p^2 - C^2)^{1/2}}{R_p}\right)\right],$$

$$\frac{\bar{A}_p}{R_p^2} = \frac{C^2}{R_p^2\left(1 - \frac{C^2}{R_p^2}\right)^{1/2}} \ln\left[1 + \left(1 - \frac{C^2}{R_p^2}\right)^{1/2}\right] + \frac{2L}{R_p}, \quad (28)$$

where C is the semiminor axis of the cap and $D_p = L + C$. It was shown by Evans (1973) that the deformed membrane cannot become spherical except for large pressures. Therefore, a spheroidal shape is a reasonable approximation that provides for the necessary difference in stress resultants T_s, T_θ over the cap surface (see Flügge [1966]).

Eqs. 27 and 28 are scaled by the pipette radius R_p; therefore for any fixed ratio of D_p/R_p, the pressure differential $(P_i - P_p)$ will be inversely proportional to the pipette radius.

$$\frac{(P_i - P_p)}{\mu} \sim R_p^{-1}. \quad (29)$$

This condition was assumed to imply a liquid interface by Rand and Burton (1964), but obviously, it is not specific to that situation.

Solving Eqs. 27 and 28 to obtain $(P_i - P_p)R_p/\mu$ as a function of D_p requires

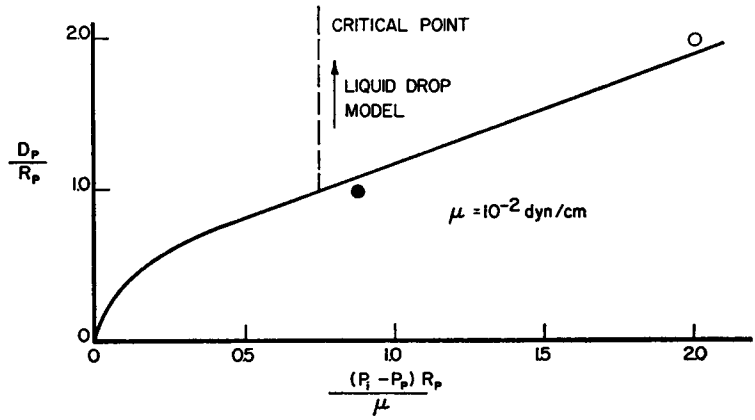

FIGURE 7 The dimensionless ratio $(P_i - P_p)R_p/\mu$, representing the pressure difference required to aspirate the cell a distance D_p into the pipette, is shown as a function of the dimensionless distance D_p/R_p. The curve illustrates the shoulder and increasing pressure characteristic beyond the $D_p/R_p = 1$ critical point. The dark circle is the average value of of $(P_i - P_p)R_p/\mu$ data (using $\mu = 10^{-2}$ dyn/cm) obtained from Dr. R. S. Heusinkveld of the Hematology Department, University of Rochester, Rochester, N. Y.; these data were all taken at $D_p = R_p$. The open circle is the average value of D_p/R_p data for a fixed $(P_i - P_p) = 3$ mm H_2O (again using $\mu = 10^{-2}$ dyn/cm) obtained from Dr. P. F. Leblond of the Institut de Pathologie Cellulaire, Paris.

definition of the value C at which the cylindrical section begins to form. The cap height C must be less than R_p. In order to establish C (and $L = D_p - C$), the minimum value of $(P_i - P_p)R_p/\mu$ is found for a given D_p and variable C. Exact solution of Eq. 27 requires solution of Eqs. 13, 16, and the incompressibility relation, but is not necessary here.

Fig. 7 is a plot of $(P_i - P_p)R_p/\mu$ vs. D_p. The curve illustrates the shoulder and increasing pressure characteristics observed by Rand and Burton (1964) beyond the critical point $D_p = R_p$. At this point,

$$(P_i - P_p) = (0.75\ \mu)R_p^{-1}.$$

Using the data of Rand and Burton (1964), the value of the elastic constant μ is from 1 to 5×10^{-2} dyn/cm and the equivalent modulus of elasticity 1 to 5×10^4 dyn/cm^2. Some recent work of Heusinkveld and Leblond is shown in Fig. 7 that yield a value of 10^4 dyn/cm^2 for the equivalent shear modulus.[2] Another interesting observation (corroborated by our experiments) is that the linear stress-strain law is good for large strains ($\lambda_s = 2$ or $\epsilon_s = 150\%$), which supports the two-dimensional elastomer concept. Fig. 8 shows the extension ratio λ_s at the pipette tip as a function of D_p/R_p.

[2] Dr. P. F. Leblond of the Institute de Pathologie Cellulaire, Paris, and Dr. R. S. Heusinkveld of the Hematology Department, Rochester University, Rochester, N. Y., have kindly provided recent data using improved measurement techniques and many helpful suggestions.

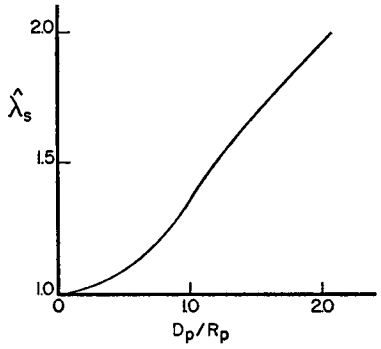

FIGURE 8 The extension ratio $\hat{\lambda}_s$ at the pipette tip is plotted as a function of the dimensionless distance D_p/R_p.

Rand (1964) estimated the modulus of elasticity at $10^7 - 10^8$ based on hemolysis of osmotically swollen cells using the micropipette. Here, the interpretation is that the membrane tension is very large such that the shear deformation can be ignored. Using Rand's data, the value for $-p_M$ would be from 10 to 25 dyn/cm at the yield point. The equivalent modulus of elasticity would be at least the order of 10^7 dyn/cm^2. Indeed, the value would be more in the range of 10^9 or greater when one considers the small area dilation at lysis. This modulus corresponds to the "bulk" modulus whereas μ corresponds to the shear modulus by analogy with ordinary materials. The bulk modulus by these measurements is three to five orders of magnitude greater than the shear modulus; therefore, the initial assumption of two-dimensional incompressibility would be valid.

CONCLUSIONS

Two mechanical experiments on red blood cells were analyzed: fluid shear deformation of point-attached red cells, and micropipette aspiration of red cell discocytes. The elastic constant corresponding to the shear modulus was found to be of the order 10^{-2} dyn/cm or 10^4 dyn/cm^2 for the equivalent modulus in both cases. The large modulus estimated by Rand (1964) and Katchalsky et al. (1960), 10^8–10^9 dyn/cm^2 corresponds to the bulk modulus of the material and supports the incompressibility hypothesis because it is significantly greater than the shear modulus. The two-dimensional, incompressible material correlates with additional experimental observations: the tether or microfilament and teardrop formation for attached red cells; the increasing pressure difference beyond the critical cap formation in micropipette aspiration of red cells; and consistency with the formation of a pinch off globule in micropipette experiments. The linear form of the stress-strain law correlates with experiment for large strains.

These correlations provide strong support for the proposed material character and and imply molecular structure in the plane of the membrane that has been generally

neglected. However, there is evidence (Blais and Geil, 1969) obtained from electron micrographs of stretched red cell ghosts that long molecular chains can be observed aligned with the direction of stretch. This is compatible with the molecular concept of a two-dimensional, incompressible material (Evans, 1973): randomly kinked, and cross-linked chains that are elongated and oriented upon stretching, decreasing entropy content. The material is the two-dimensional analogue of a weak elastomer. The specific questions concerning the roles played by protein and phospholipid need to be investigated. In addition, the dependence on metabolic processes (e.g., the case of ATP depletion) may be significant (Weed and LaCelle, 1969). If the protein component of the composite membrane is the primary elastomeric element (forming a matrix foundation with the phospholipid existing interstitially), another interesting phenomenon could be explained. Red cells sphere and spawn small spherical "buds" when they are heated to 55°C. At this temperature, the protein can denature causing the membrane to lose its structural integrity. A sample calculation of molecular weight for the structural subunit, using the shear modulus, is contained in the Appendix.

The author gratefully acknowledges the support of the Medical Research Council of Canada through grant no. MA-5055.

Received for publication 26 February 1973.

REFERENCES

BLAIS, J. J. B. P., and P. H. GEIL. 1969. *Biopolymers.* 8:275.
EVANS, E. A. 1973. *Biophys. J.* 13:926.
FLÜGGE, W. 1966. Stresses in Shells. Springer-Verlag New York Inc., New York. 23, 78.
FUNG, Y. C., and P. TONG. 1968. *Biophys. J.* 8:175.
HOCHMUTH, R. M., and N. MOHANDAS. 1972. *J. Biomech.* 5:501.
KATACHALSKY, A., O. KEDEM, C. KLIBANSKY, and A. DEVRIES. 1960. *In* Flow Properties of Blood and Other Biological Systems. A. L. Copley and G. Stainsby, editors. Pergamon Press, New York.
MARCHESI, V. T., E. STEERS, T. W. TILLACK, and S. L. MARCHESI. 1969. *In* Red Cell Membrane. G. A. Jamieson and T. J. Greenwalt, editors, J. B. Lippincott Company, Philadelphia. 117.
MEARES, P. 1967. Polymers: Structure and Bulk Properties. D. Van Nostrand Co. Ltd., London. 205.
MITCHISON, J. M., and M. M. SWANN. 1954. *J. Exp. Biol.* 31:443.
PRAGER, W. 1961. Introduction to Mechanics of Continua. Ginn and Company, Boston. 188, 198, 206, 208, 209, 211.
RAND, R. P. 1964. *Biophys. J.* 4:303.
RAND, R. P., and A. C. BURTON. 1964. *Biophys. J.* 4:115.
SKALAK, R., A. TOZEREN, R. P. ZARDA, and S. CHIEN. 1973. *Biophys. J.* 13:245.
WEED, R. I., and P. L. LACELLE. 1969. *In* Red Cell Membrane. G. A. Jamieson and T. J. Greenwalt, editors, J. B. Lippincott Company, Philadelphia. 318.

APPENDIX

A simple statistical thermodynamic calculation can be used to relate the shear modulus to the molecular weight of a subchain in the network (see Meares [1967]).

$$\mu/t_m \simeq \nu kT$$

where ν is the number of subchains per unit volume; k is the Boltzmann constant; T is temperature; and t_m is the membrane thickness. The chain density is given by,

$$\nu = \rho(N_A/M_W),$$

where ρ is the density; N_A is Avogadro's number; and M_W is molecular weight. Using the value of $\mu/t_m = 10^4$ dyn/cm², the molecular weight of the subchain would be of the order 10^5. This is the same magnitude as the fibrous protein, "spectrin," that has been isolated from the red cell membrane by Marchesi et al. (1969).